Modeling and control of dissolved oxygen concentration in the fermentation of Glucose to Gluconic Acid

Abstract

Fermentation systems are often highly nonlinear, with poorly understood dynamic behaviour of the reactor. In this work, mathematical modeling of the fermentation process based on aeration rate control was performed in a semi-batch airlift loop bioreactor. The bioconversion of glucose to gluconic acid by the Aspergillus niger strain was considered in an oxygen consuming system in the liquid phase. The proper kinetic model for the bioconversion of glucose to gluconic acid was investigated using experimental data from a 40 dm³ reactor. Kinetic parameter estimation was used from the literature. The model was validated by experimental data and was compared with the Monod kinetic model. The comparison showed that the Contois kinetic model was in a better agreement with the experimental data of dissolved oxygen concentration (DO) than the Monod kinetic model. An optimal substrate-to-microorganism concentration ratio of 55 was suggested by applying the model, which led to achieving the maximum conversion of glucose to gluconic acid. The conventional PID controller with fixed parameters obtained from the Ziegler-Nichols tuning method was used to control the dissolved oxygen concentration at a constant level of 2 mg/dm³, which was important for microorganism survival and growth.

Keywords

Modeling · Contois kinetic · Dissolved oxygen · Fermentation · Bioreactor · PID Controller

Mohammad Amin Kazemi

Department of Chemical and Petroleum Engineering, Sharif University of Technology, Azadi Avenue, P.O. Box 11365-9465 Tehran, Iran
e-mail: amin_kazemi@che.sharif.ir

Hanieh Bamdad

Department of Chemical Engineering, Shahid Bahonar University of Kerman, P.O. Box 7616914111, Kerman,, Iran

Sadegh Papari

Department of Chemical and Petroleum Engineering, Sharif University of Technology, Azadi Avenue, P.O. Box 11365-9465 Tehran, Iran

Soheila Yaghmaei

Department of Chemical and Petroleum Engineering, Sharif University of Technology, Azadi Avenue, P.O. Box 11365-9465 Tehran, Iran
e-mail: yaghmaei@sharif.edu

1 Introduction

Gluconic acid (GLA) is a mild organic acid compound with a wide applicability, which is produced from glucose oxidation. This compound has been used in industrial products such as detergents, leather, photography, textiles, pharmaceuticals and especially food. There are different methods for manufacturing gluconic acid, including chemical methods, electrochemical methods, enzyme bioreactors, as well as free or immobilised cells of either *Gluconobacter oxydans* or *Aspergillus niger* (Rao et al., [18]; Roehr et al., [19]; Sahasrabudhe and Sankpal, [20]). Among these methods, producing gluconic acid with *Aspergillus niger* microbe is preferable due to the easier isolation of the product compared to other biocatalysts. Such isolation could be carried out by flocculation with polyelectrolytes (Lee and Long, [10]), covalent binding to a glycidyl ester copolymer (Nelson, [15]), entrapment in gels (Garg and Sharma, [6]) and adsorption onto supports (Heinrich and Rehm, [7]; Sakurai et al., [21]; Fujii et al., [5]). On the other hand, producing gluconic acid from glucose using metal catalysts, regardless of the high conversion and selectivity, creates its own problem of catalyst deactivation, which is caused by self-poisoning and overoxidation (Nikov and Paev, [16]).

The reaction of glucose conversion to gluconic acid by *Aspergillus niger* needs a high amount of dissolved oxygen either for bioconversion of glucose into gluconic acid or mycelia respiration. For this purpose, airlift loop reactors are appropriate because of a high mass transfer rate between gas and liquid phases compared to the other types of reactors. The advantages of such reactors to stirred tank ones are simplicity, lower energy consumption, easier maintenance and lower shear stress (Braun and Vecht, 1991 [2]) which may cause damage to microorganisms. Airlift loop reactors were used for the first time by Lefrancois et al. [12]. Since then, a wide range research has been conducted on kinetic modeling and the microbial reaction yielding gluconic acid. Luttman et al. [13] evaluated the reaction kinetics using a model of tanks in series. Znad et al. [24] studied the reaction kinetics in a batch reactor. Sikula et al. [22] investigated glucose to gluconic acid production by utilising the tank in series model with Monod kinetics. Lavric and Muntean [9]

also studied GLA production using the Monod kinetic model; they considered axial dispersion for the liquid phase.

Despite these extensive studies, the mathematical modeling of airlift loop bioreactors with simultaneous dissolved oxygen control has not been studied. During the fermentation process, the amount of oxygen required by the microorganisms to be able to oxidise the organic substance and also the required oxygen to maintain the DO concentration above its critical value should be supplied by the aeration system. At high cell concentrations, the amount of consumed oxygen may exceed the rate of oxygen transfer from the gas bubbles, which in turn may lead to depletion of oxygen. Therefore, the DO concentration in the reactor is one of the most important controllable operating parameters during the bioconversion which affects the process efficiency and operating costs. Since fermentation processes are usually highly nonlinear, a deviation from the operating region close to the designed conditions can significantly degrade the controller performance and system instability. The key innovation of this paper is the use of an electronic controller to keep the dissolved oxygen concentration at an adequate value of 2 mg/dm^3.

There are three general methods of controlling DO in a fermentation process. One is on the basis of manipulating the agitation speed to improve mass transfer. The second is based on changing the oxygen partial pressure in the inlet gas and the third way is adjusting the air flowrate. In this study, the manipulation of air flowrate was selected as the method of controlling dissolved oxygen concentration due to the fact that it is simpler to be applied in industrial processes, less expensive and has higher effects on oxygen transfer rate compared to the other methods. In the present work, we applied a mathematical model for producing gluconic acid by *Aspergillus niger* in a semi-batch airlift loop reactor by considering an axial dispersion for liquid phase. Moreover, the Contois kinetic model was used for the determination of reaction parameters used in the model. Since precise evaluation of ALR reactors behaviour is difficult, and the experimental investigation on these kinds of reactors are expensive and time consuming (Onken and Weiland, [17]; Merchuk and Scuger, [14]), there is a need to perform a mathematical model which enables us to evaluate the effects of circulation rate, downcomer to riser diameter ratio, operational pressure and the height to reactor diameter ratio on GLA production. Also, the optimal concentration of the substrate to the concentration of microorganisms that leads to maximum conversion can be estimated mathematically.

2 Modeling mathematics

An overall schematic of the model is represented in Fig. 1. ALR reactors can be considered as consecutive small stirred tanks in series to calculate the mass transfer coefficient (Chisti, [3]). However, subsequent studies have not been conducted to confirm the reliability of such a simple assumption for industrial large scale reactors [1].The top of the riser can be considered as part of the riser extension (Dhaouadi et al., [4]). The mass balance in the liquid phase is then as follows:
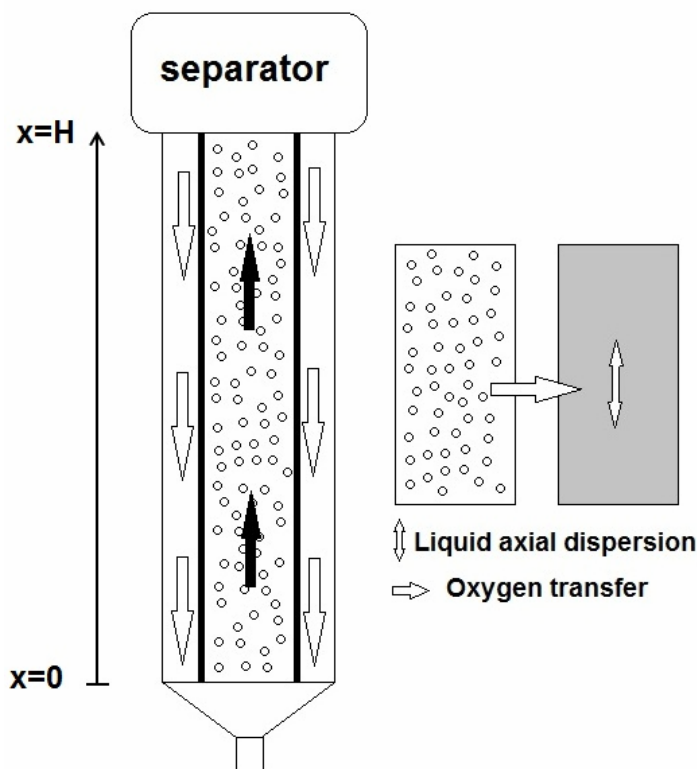
Fig. 1. Schematic diagram of the Axial Dispersion model for an Airlift loop bioreactor

ance in the liquid phase is then as follows:

$$\frac{\partial C_{\text{liq},i}}{\partial t} = D_{\text{ax}} \frac{\partial^2 C_{\text{liq},i}}{\partial x^2} - \frac{U_{\text{liq}}}{1-\varepsilon} \frac{\partial C_{\text{liq},i}}{\partial x} + r_i \qquad i = M, P, S \quad (1)$$

where M, P and S represent microorganism, product, substrate concentrations, respectively. Since the oxygen exists in both liquid and gas phases, the mass balance equation for this component differs from the other three components and is written as:

$$\frac{\partial C_{\text{liq},O_2}}{\partial t} = D_{\text{ax}} \frac{\partial^2 C_{\text{liq},O_2}}{\partial x^2} - \frac{U_{\text{liq}}}{1-\varepsilon} \frac{\partial C_{\text{liq},O_2}}{\partial x} + \\ + \frac{1}{1-\varepsilon} k_l a (C_{\text{liq},O_2} - C_{\text{liq},O_2}) + r_i \qquad (2)$$

The energy balance was not considered in the mathematical modeling since the fermentation process occurs so slowly that the bioreactor's temperature remains almost constant.

To avoid complicated coupled differential equations, it is reasonable to assume that the gas velocity decreases proportionally to the reaction conversion while rising through the reactor. Therefore, it can be obtained in each section of the riser section as follows:

$$U_g = U_0 (1 + \varepsilon_A x_{\text{con}}) \qquad (3)$$

where U_g (m/s) is the gas velocity in the reactor and U_0(m/s) is the inlet gas velocity. The parameter ε_A is the volume expansion factor. For constant temperature and density, it can be defined as:

$$\varepsilon_A = \frac{V_{x_{\text{con}}=1} - V_{x_{\text{con}}=0}}{V_{x_{\text{con}}=0}} \qquad (4)$$

Mohammad Amin Kazemi / Hanieh Bamdad / Sadegh Papari / Soheila Yaghmaei

The overall gas holdup and oxygen mass transfer coefficient was obtained by the following equations (Jurascik et al., [8]):

$$\varepsilon = 0.946 \left(1 + \frac{A_D}{A_R}\right)^{-1} U_g^{0.667} \qquad (5)$$

$$k_l a = 0.428 \left(1 + \frac{A_D}{A_R}\right)^{-1} U_g^{0.8} \qquad (6)$$

For the axial dispersion coefficient of the liquid phase, Towell and Ackermann [23] found:

$$D_{\text{ax}} = 2.61 D_R^{1.5} U_g^{0.5} \qquad (7)$$

3 Reaction model and kinetics

The overall reaction of bioconversion of glucose into gluconic acid can be considered as follows:

$$C_6H_{12}O_6 + \frac{1}{2}O \rightarrow C_6H_{12}O_7$$
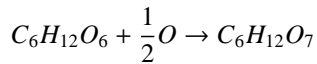
The rate equation for microorganism based on the Contois kinetic model and by assuming biomass inhibition is:

$$\frac{dM}{dt} = \mu_m \frac{S}{K_S M + S} \frac{C_{\text{liq},O_2}}{K_O M + C_{\text{liq},O_2}} M \qquad (8)$$

while for the Monod kinetic model it can be obtained by the following equation:

$$\frac{dM}{dt} = \mu_m \frac{S}{K_S' M + S} \frac{C_{\text{liq},O_2}}{K_O' M + C_{\text{liq},O_2}} M \qquad (9)$$

Other components' concentrations can then be calculated by the following equations:

$$\frac{dP}{dt} = \alpha \frac{dM}{dt} + \beta M \qquad (10)$$

$$\frac{dS}{dt} = -\gamma \frac{dM}{dt} - \lambda M \qquad (11)$$

$$\frac{dO_2}{dt} = -\delta \frac{dM}{dt} - \phi M \qquad (12)$$

The initial concentrations of substances are:

$$M(x,0) = M_0 \qquad (13)$$

$$P(x,0) = 0 \qquad (14)$$

$$S(x,0) = S_0 \qquad (15)$$

$$C_{\text{liq}}(x,0) = C_{\text{liq}}^* \qquad (16)$$

The boundary values are:

$$at\,x = H \rightarrow \frac{\partial C_{\text{liq},t}}{\partial x} = 0 \quad t = M, P, S, O_2 \qquad (17)$$

$$at\,x = 0 \rightarrow C_{\text{liq},i}^{\text{downcomer}}(H,t) = C_{\text{liq},i}^{\text{riser}} \quad t = M, P, S, O_2 \qquad (18)$$

The kinetic parameters and operational conditions used in mathematical modeling are summarised in Table 1 and Table 2, respectively.

At each time step, the error can be calculated by the difference between the set point and the measured value.

$$e(t) = \text{set point} - \text{measured value} \qquad (19)$$

The controller output is calculated by summing up the three-term control: the proportional, integral and derivative values, denoted in Eq. (20) by the subscripts P, I, and D:

$$u(t) = K_P e(t) + \frac{1}{\tau_I} \int_0^t e(\tau)\,d\tau + \tau_D \frac{de(t)}{dt} \qquad (20)$$

In order to obtain the controller output, $u(t)$, the integral and differential terms should be solved numerically in each time step. In this work, the former was obtained from trapezoidal rule, while finite difference formula was used to calculate the latter.

4 Results and discussion

By simultaneously solving mass conservation equations for all components and applying the initial and boundary conditions, the microorganism, glucose, oxygen and gluconic acid concentrations were obtained during the reaction time. Fig. 2 illustrates a comparison between the axial dispersion-Contois model, the tank in series-Monod model and the experimental data from Sikula et al. [22]. The dissolved oxygen concentration can be measured with an optical DO sensor, which is situated at the bottom of the reactor. The oxygen concentration decreased over time because it was consumed for the conversion of glucose and was required by microbes as well for growth and survival.

The experimental and also simulated results showed that the microorganism concentration starts from 0.146 g/dm³, and then increased gradually as they consumed substrate and oxygen during the fermentation, and finally, reached to the asymptotic value of 6 g/dm³.

As is apparent from Fig. 2, the Contois kinetic model with considering the axial dispersion for the liquid phase has a better coherence with the experimental data compared to the Monod kinetic model with considering the reactor as N-tanks in series. For the case of oxygen (Fig. 2d), the difference between these two models is more significant, which means that the Monod model fails to predict the dissolved oxygen concentration in fermentation of glucose to gluconic acid.

Also, the results showed that the DO concentration in the reactor dropped to lower than 2 mg/dm³ in the absence of the controller, which reflects the need for a controller to maintain the oxygen concentration on the desired value. The concentrations of dissolved oxygen along the reactor (Riser and Downcomer) for three typical times of operation are shown in Fig. 3. As it is obvious from the Figure, the concentrations do not change significantly with axial direction. This is mainly due to the circulation of the liquid products with a velocity of about 1 m/s in the reactor. Therefore, the reactor operates more similar to a well-mixed reactor rather than a plug flow one. However, the mathematical modeling has to be performed such general that can cover a wide variety of operation conditions. As an example, let's consider a case in which it is required to lower the liquid circulation velocity to reduce the power consumption. Here, the reactor may not operate in the "well-Mixed" region anymore

Tab. 1. Estimated kinetic parameters by Sikula et al. [22]

$\mu_m(h^{-1})$	K_O	K_S	α	$\beta(h^{-1})$	γ	$\lambda(h^{-1})$	δ	$\phi(h^{-1})$
0.316	0.001061	21.447	2.58	0.1704	2.1768	0.2937	0.2724	0.0425

Tab. 2. Geometric details and operational conditions

U_g(m/s)	U_{liq}(m/s)	D_R(m)	H(m)	Pressure(bar)	T(˚C)	M_0(g/dm^3)	S_0(g/dm^3)
0.11	1.0	0.106	1.93	1	30	0.146	150
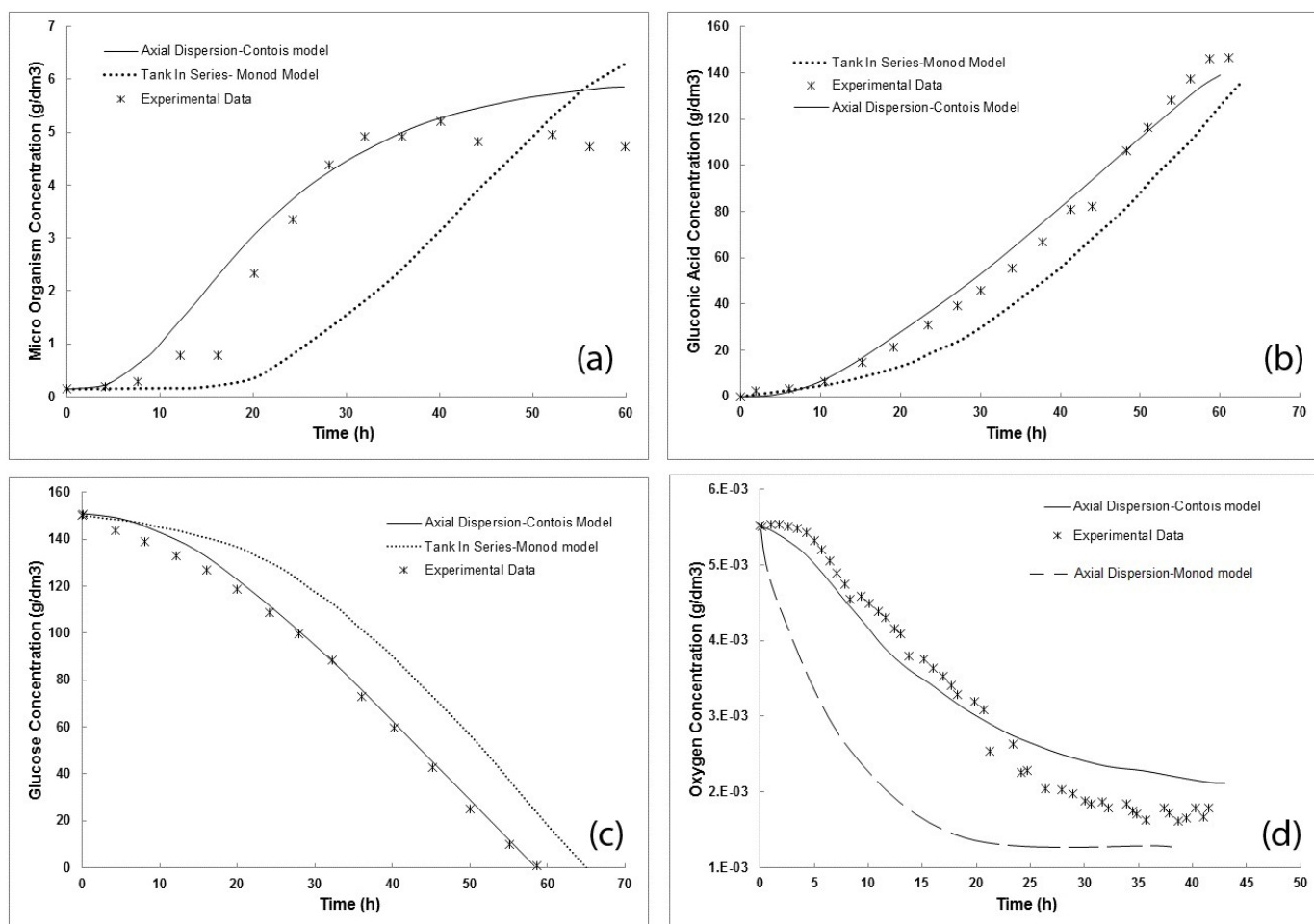
Fig. 2. Model vs. experimental data measured in the 40 dm^3 ALR (Sikula et al., [22])

and may show a behavior between completely mixed and plug reactor. Thus, choosing the axial dispersion model which is flexible to the change in the flow regime would be a good choice.
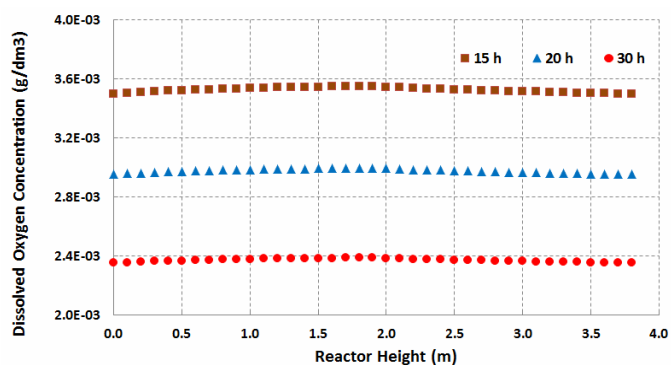
Fig. 3. Variation of Dissolved Oxygen Concentration along the reactor (the distance from 0 to1.93 m is considered as the riser section and 1.93 m to 3.86 m is supposed to be the downcomer section)

4.1 Effect of air flowrate on gluconic acid production

The concentration of gluconic acid at different gas velocities is shown for 24 hours of fermentation in Fig. 4.

As the figure indicates, by increasing the gas velocity up to 0.1 m/s, GLA production increased considerably, but with gas velocities higher than 0.25 m/s, the gas flowrate had insignificant effects on GLA production. This could be due to the fact that at high gas flowrates, the mass transfer resistance is reduced and the kinetic resistance may determine the amount of GLA production.

Fig. 5 shows the GLA concentration with reaction time for different gas velocities. Although an increase in gas velocity had minor effects on the final production value, it had a considerable effect on the reaction termination time. It must be noted that an excessive increase in the gas flowrate led to greater shear stress which can cause cell damage and a reduction in GLA production.

Mohammad Amin Kazemi / Hanieh Bamdad / Sadegh Papari / Soheila Yaghmaei
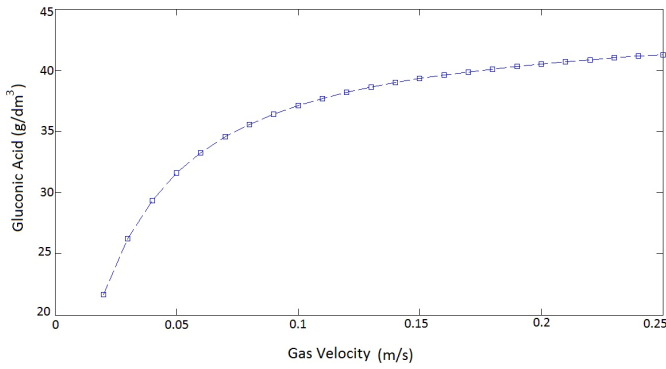
Fig. 4. Effect of gas velocity on GLA concentration after 1 day of fermentation.
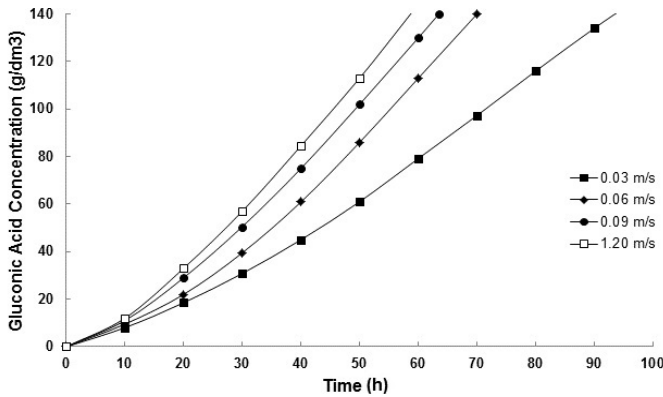
Fig. 5. Effect of gas velocity on GLA production rate for a 40 dm³ ALR.

4.2 Effect of pressure on GLA formation

Some researchers have evaluated the positive effect of an elevation in operational pressure on the efficiency of glucose to gluconic acid bioconversion (Sakurai et al., [21], Lee et al., [10]). Fig. 6 shows the effects of operational pressure on GLA concentration with time. According to the figure, by increasing pressure, more oxygen can dissolve in the liquid phase, leading to increased GLA production and, subsequently, a shorter reaction termination time.
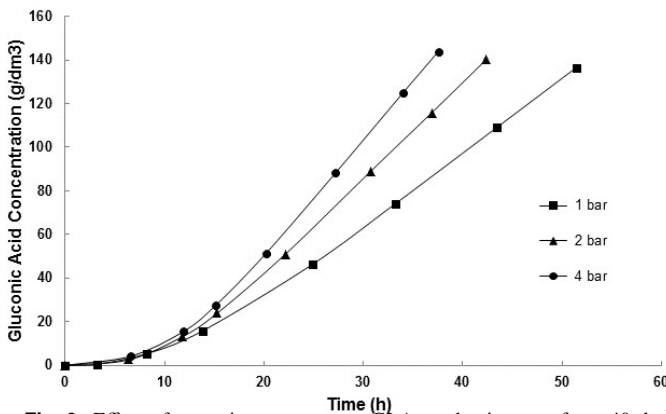
Fig. 6. Effect of operating pressure on GLA production rate for a 40 dm³ ALR.

In general, the solubility of oxygen depends on its partial pressure and the water temperature. The amount of dissolved oxygen concentration (ppm) in water at different pressures and temperatures is shown in Table 3.

Tab. 3. Oxygen solubility in water at different pressures and temperatures (ppm)

Temperature (˚C)	1 bar	2 bar	4 bar
10	11.3	22.6	45.1
20	9.1	18.2	36.4
30	7.6	15.2	30.3

4.3 Effect of reactor geometry and circulation rate on GLA production

The effect of downcomer to riser diameter on the production rate is shown in Fig. 7. As is clear, by increasing the downcomer to riser area ratio, reaction termination time was reduced. However, this did not have a considerable effect. Based on these results, the higher the D_R/D_D, the higher the mass transfer occurs between the gas and liquid phases according to Eq. (6 which in turn leads to having more dissolved oxygen and increased GLA production rate.
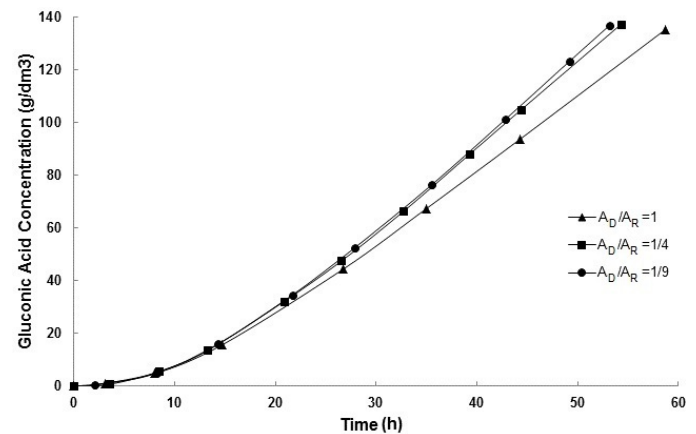
Fig. 7. Effect of downcomer to riser area ratio on GLA production rate.

Moreover, the computer simulation shows that changing the ratio of the reactor length to the reactor diameter and also the liquid circulation rate had no significant effect on the final reaction period and production efficiency. These results indicate that the airlift loop tank may behave almost as a perfectly mixed reactor. To show the validity of this statement, the concentration of the dissolved oxygen along the riser and downcomer is depicted in Fig. 8. As is seen from the Figure, the concentration of dissolved oxygen increases in the riser until it reaches to a maximum point. Then the oxygen concentration starts to decrease as the liquid moves down through the downcomer. This is due to the fact that the reaction is still taking place and consuming oxygen in the downcomer, while there is no aeration in this section. Nevertheless, this variation in dissolved oxygen concentration is significant enough to assume the reactor almost acts as a perfectly mixed one. Another point which is important to note from the Fig. 8 is that the lowest oxygen concentration is found at the bottom, which suggests that the optical DO sensor should be installed at this point to show the minimum value of dissolved oxygen during the fermentation.

4.4 Application of the model for optimisation

Although the glucose to gluconic acid reaction is relatively a high conversion reaction, however, for establishing a higher conversion rate of glucose at a specific temperature, pressure and gas velocity, an optimal ratio of the substrate to the initial microorganism concentration was obtained by mathematical modeling.

As Fig. 8 shows, starting the reaction with a ratio of $S_0/M_0 = 55$ leads to the highest conversion of the substrate equal to 94.8% and consequently the maximum GLA production.
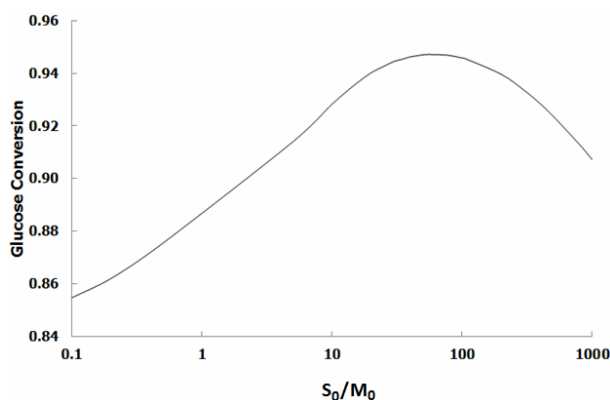
Fig. 8. Effect of initial substrate to microorganism concentration on the conversion of the reaction. The reactor volume is 40 dm^3.

4.5 Controlling dissolved oxygen concentration

A schematic representation of the DO control system is shown in Fig. 9. The oxygen concentration was measured by a DO sensor which was situated near the bottom of the reactor since the minimum amount of oxygen presents at the bottom. To provide aeration, an air compressor can be used which is connected to an electric control valve. In practical applications, the dissolved oxygen concentration in the reactor should be maintained in the range of 1.5-4 mg/dm^3. A value of 2 mg/dm^3 is commonly used, as values above 4 mg/dm^{3}do not have a significant effect on operation and can increase aeration costs. The aim of this work was to maintain the oxygen concentration at 2 mg/dm^3. The air flowrate was examined as the manipulated variable because of simpler operation and lower operating costs. In the cases where the controller commands were negative, the air valve started to be closed automatically and remained closed until another positive signal is supplied from the controller. A conventional PID controller with fixed parameters ($K_c = 0.684$, $\tau_I = 255s$, $\tau_D = 29.95s$) was used to maintain the DO level at the desired value. The PID parameters were obtained from the Ziegler-Nichols tuning method.

As the reaction proceeded, the dissolved oxygen decreased until it reached the set point value. To test the PID controller performance, three different set points with negative and positive step changes were applied (Fig. 10). As can be seen from the figure, the PID controller succeeded in maintaining the dissolved oxygen at the desired value and showed good dynamic
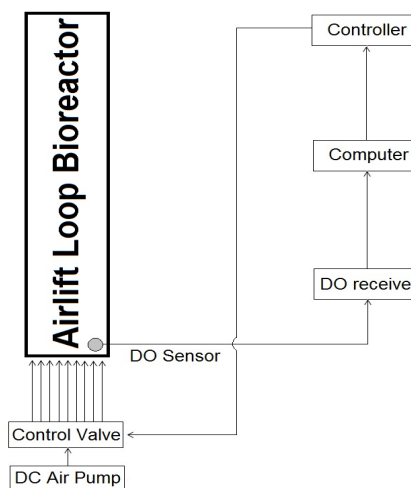
Fig. 9. Schematic view of the dissolved oxygen control process.

performance in terms of DO concentration control about the set point.

When the DO level dropped below 2 mg/dm^3, the gas flowrate started to increase and the on-line PID controller system kept the dissolved oxygen concentration at the set point (Fig. 11a). Although the oxygen concentration approached a certain value, however, the gas flowrate did not reach the steady state condition (Fig. 11b). This can be attributed to the need of growing microorganisms for oxygen as long as adequate substrate exists in the reactor.
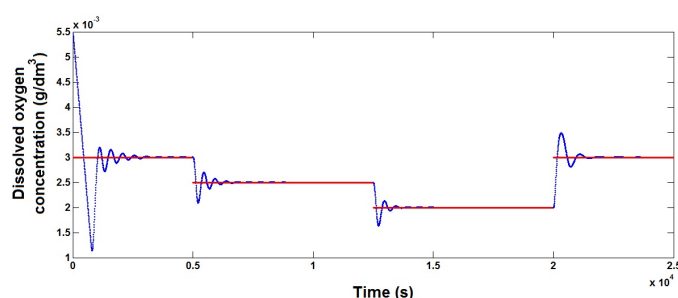
Fig. 10. The dissolved oxygen concentration for positive and negative step changes in set point.

Conclusion

Gluconic acid production using immobilised *A. niger* in a recirculation bioreactor was investigated using unsteady state conditions for the consumption of dissolved oxygen by microbes and the reaction. The dynamic behaviour of the bioreactor was studied by mathematical modeling of the reactor. The results of the numerical simulation had a good consistency with experimental data from the literature. As the mathematical model showed, the Contois model with axial dispersion provided a better estimation of the experimental dissolved oxygen concentration compared to the Monod kinetic model. Also, it was observed that the rate of GLA production strongly depended on the gas flowrate and operational pressure. However, the liquid circulation rate and the riser to downcomer diameter ratio did not have a significant effect on reaction efficiency. Moreover, it
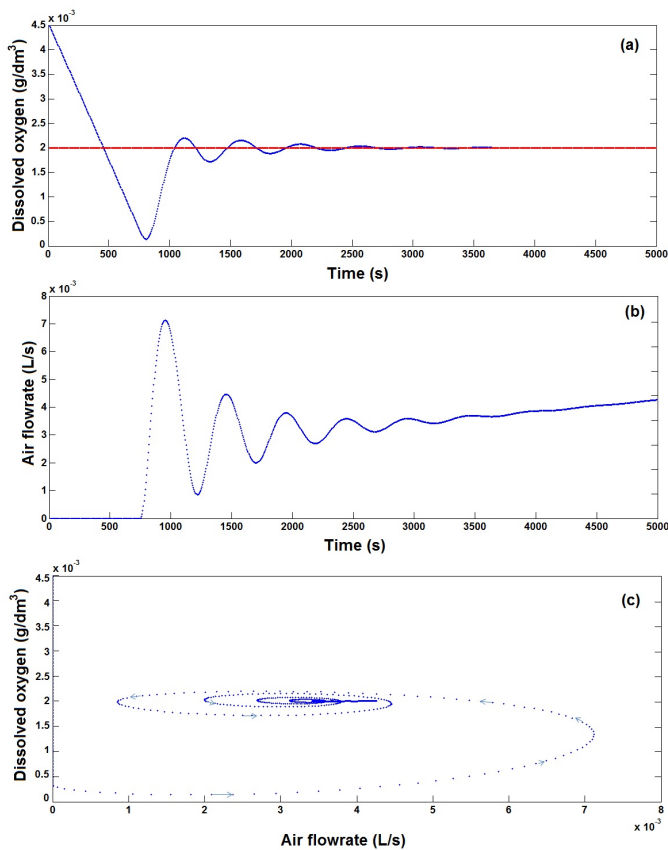
Fig. 11. PID control of the bioreactor. (a) Changes in dissolved oxygen concentration with time. (b) Changes in the manipulated variable (air flowrate) with time. (c) Changes in dissolved oxygen concentration with variation of the manipulated variable.

can be concluded that starting the reaction with a substrate-to-microorganism concentration ratio of 55 maximized the conversion of glucose to gluconic acid.

DO concentration control is a difficult task in batch fermentation due to the varying reaction conditions over time and with instrument time delays. However, controlling the DO concentration in the bioconversion of glucose to gluconic acid with a PID controller was implemented and satisfactory results were obtained for the DO level in the growth medium.

Notations

A cross section area, m^2

ALR airlift loop reactor

C concentration, g/dm^3

D diameter, m

D_{ax} axial dispersion coefficient, m^2/s

DO Dissolved Oxygen

$e(t)$ error, g/dm^3

H height, m

$k_l a$ volumetric mass transfer coefficient, h^{-1}

K_O Contois oxygen limitation constant for the microorganism, dimensionless

K'_O Monod oxygen limitation constant for the microorganism, dimensionless

K_p proportional gain, dimensionless

K_S Contois saturation constant for the microorganism, dimensionless

K'_S Monod saturation constant for the microorganism, dimensionless

Q gas flowrate (dm^3/s)

Q_0 inlet gas flowrate (dm^3/s)

r_i rate of reaction for component i, g/dm^{3}h

t time, h

u controller output

U_g gas velocity, m/s

U_L liquid circulation rate, m/s

x axial coordinate, m

S Substrate concentration, g/dm^3

S_0 Initial substrate concentration, g/dm^3

x_{con} the conversion of the reaction

M Microorganism concentration, g/dm^3

M_0 Initial microorganism concentration, g/dm^3

P Product concentration, g/dm^3

Greek letters

α growth associated glucose consumption coefficient, dimensionless

β non-growth associated glucose consumption coefficient, dimensionless

γ growth associated oxygen consumption coefficient, dimensionless

λ substrate mass consumed per microorganism mass grown per hour, h^{-1}

δ non-growth associated oxygen consumption coefficient, dimensionless

ϕ oxygen mass consumed per microorganism mass grown per hour, h^{-1}

ε hold-up, dimensionless

τ_D derivative time, s

τ_I integral time, s

ε_A volume expansion factor, dimensionless

μ_m maximum specific growth rate, h^{-1}

Subscripts

D downcomer

g gas

i compound i (substrate, product, microorganism, oxygen), dimensionless

liq liquid

O_2 oxygen

R riser

$*$ equilibrium

0 initial

References

1 **Blazej M, Annus J, Markos J**, *Comparison of gassing-out and pressure step dynamic methods for k_LA measurement in an airlift reactor with internal loop*, Chem. Eng. Res. Des., **82 (A10)**, (2004), 1375–1382.

2 **Braun S, Vecht-Lifshitz S**, *Mycelia morphology and metabolite production*, Trends Biotechnol., **9**, (1991), 63–68.

3 **Chisti MY**, *Airlift Bioreactors*, Elsevier Applied Science; New York, 1989.

4 **Dhaouadi H, Poncin S, Midoux N, et al.**, *Gas-liquid mass transfer in an airlift reactor-analytical solution and experimental confirmation*, Chem. Eng. Process., **40**, (2001), 129–133.

5 **Fujii N, Yasuda K, Sakakibara M**, *Effect of volume ratio of cellulose carriers and time interval of repeated batch culture on citric acid productivity by immobilized Aspergillus niger*, J. Ferment. Bioeng., **78**, (1994), 389–393.

6 **Garg K, Sharma CB**, *Continuous production of citric acid by immobilized whole cells of Aspergillus niger*, J. Gen. Appl. Microbiol., **38**, (1992), 605–615.

7 **Heinrich M, Rehm HJ**, *Formation of gluconic acid at low pH values by free and immobilized Aspergillus niger cells during citric acid fermentation*, Eur. J. Appl. Microbiol. Biotechnol., **15**, (1982), 88–92.

8 **Jurascik, Blazej M, Annus J, Markos J**, *Experimental measurements of volumetric mass transfer coefficient by the dynamic pressure-step method in internal loop airlift reactors of different scale*, Chem. Eng. J., **125**, (2006), 81–87.

9 **Lavric V, Muntean O**, *Experimental measurements of volumetric mass transfer coefficient by the dynamic pressure-step method in internal loop airlift reactors of different scale*, Rev. Chem., **38**, (1987), cited Uzumaki, T., Kawase, Y.: *Modeling and scale up of airlift bioreactors*, 3rd German/Japanese symposium bubble column (1994), 807–814.

10 **Lee C, Long M**, *US Patent*, 1974, Patent No.:3, 821, 86.

11 **Lee HW, Sato S, Mukataka S, Takahashi J**, *Studies on the production of gluconic acid by Aspergillus niger under high dissolved oxygen concentration*, Hakkokogaku, **65**, (1987), 501–506.

12 **Lefrancois L, Mariller CGT, Mejane JV**, *Effectionnements aux Procedes de Cultures Forgiques et de Fermentations Industries Brevet D'Invention*, 1955, pp. 102–200. Delivree le 4 Mai.

13 **Luttman R, Thoma H, Buchholz K, Schugerl K**, *Model development, parameter identification, and simulation of SCP production processes in airlift reactor with external loop*, Comput. Chem. Eng., **7**, (1983), 43–50.

14 **Merchuk JC, Scuger K, Buchholz K**, *Biotechnology*, 2nd, VCH; Weinheim, 1993.

15 **Nelson M**, *Immobilized microbial cells*, 1976, Patent No.:3, 957, 580.

16 **Nikov I, Paev K**, *Palladium on alumina catalyst for glucose oxidation: reaction kinetics and catalyst deactivation*, Catal. Today, **24**, (1995), 41–47.

17 **Onken U, Weiland P**, *Airlift Fermenters: Construction, Behavior, and Uses*, In: Adv. in Biotech. Proc., Vol. 1, Alan R. Liss; New York, 1983.

18 **Rao DS, Babu PSR, Satyanarayana M**, *Technology of gluconic acid production*, Indian Chem. Eng., **35**, (1995), 58–81.

19 **Roehr M, Kubicek CP, Kominek J**, *Gluconic acid*, In: **Rehm HJ, Reed G** (eds.), Biotechnology, Product of Primary Metabolism, Vol. 6, Verlag Chemic; Weinheim, 1996, pp. 347–362.

20 **Sahasrabudhe NA, Sankpal NV**, *Production of organic acids and metabolites on fungi and applications in food industry*, In: **Khachatourians GG, Arora DK** (eds.), App. Myc. and biotech., agriculture and food production, Vol. 1, Elsevier; Amsterdam, 2001, pp. 387–425.

21 **Sakurai H, Lee HW, Sato S, Mukataka S, Takahashi J**, *Gluconic acid production at high concentrations by Aspergillus niger immobilized on a non-woven fabric*, J. Ferment. Bioeng., **67**, (1989), 404–408.

22 **Sikula I, Martin J, Markoš J**, *Modeling of fermentation in an internal loop airlift bioreactor*, Chem. Eng. Sci., **62**, (2007), 5216–5221.

23 **Towell GD, Ackerman GH**, In: Proceedings of the 5th European, 2nd International Symposium Chemical React. Eng., Amsterdam, Vol. B3, 1972, pp. 1–13.

24 **Znad H, Bales V, Markos J, Kawase Y**, *Modeling of fermentation in an internal loop airlift bioreactor*, Biochem. Engin. J., **21**, (2004a), 73–81.

25 **Znad H, Blazej M, Báles V, Markos J**, *A kinetic model for gluconic acid production by Aspergillus niger*, Chem. Pap., **58**(1), (2004b), 23–28.